ELSEVIER

Inorganica Chimica Acta 224 (1994) 61–71

Inorganica Chimica Acta

Transition metal complexes with sulfur ligands CVI☆. Phosphine and azido [Fe(L)('N_HS_4')] complexes; structural characterization of the key complex [Fe('N_HS_4')]·THF (L = PMe_3, PBu_3, PMe_2Ph, $PMePh_2$, N_3^-; 'N_HS_4'$^{2-}$ = dianion of 2,2′-bis-(2-mercaptophenylthio)diethylamine)

Dieter Sellmann*, Thomas Hofmann, Falk Knoch

Institut für Anorganische Chemie der Universität Erlangen-Nürnberg, Egerlandstrasse 1, D-91058 Erlangen, Germany

Received by Editor 28 February 1994; received by Publisher 4 May 1994

Abstract

In search of model compounds exhibiting structural and functional characteristics of the active sites of nitrogenases the phosphine complexes [Fe(L)('N_HS_4')] (L = PMe_3 (**1**), PMe_2Ph (**2**), PBu_3 (**3**), $PMePh_2$ (**4**)), the azido complex (NEt_4)[Fe(N_3)('N_HS_4')] (**5**) and [Fe('N_HS_4')]·THF (**6**) were investigated as potential precursors for the synthesis of the hypothetical N_2 complex [{Fe('N_HS_4')}$_x$(N_2)] (x = 1 or 2). **1**, **2**, **3**, **5** and **6** were characterized by X-ray structure analyses. The phosphine complexes [Fe(PR_3)('N_HS_4')] have low-spin Fe(II) centers and chiral [Fe('N_HS_4')] cores. $PMePh_2$ was the bulkiest phosphine (cone angle 136°) which could be coordinated to the [Fe('N_HS_4')] fragment. The phosphine ligands are labile and rapidly substituted by CO but not by N_2. (NEt_4)[Fe(N_3)('N_HS_4')] (**5**) is an Fe(II) high-spin complex exhibiting an achiral [Fe('N_HS_4')] core and long iron–donor distances analogous to other high-spin [Fe(L)('N_HS_4')] complexes. The azido ligand is labile and could neither oxidatively nor thermally be transformed into an N_2 ligand. The amine donor in [Fe(CO)('N_HS_4')] was deprotonated and subsequently alkylated yielding the achiral low-spin complex [Fe(CO)('$N_{Me}S_4$')]. [Fe('N_HS_4']·THF (**6**) forms a kind of intermediate between high-spin and low-spin complexes, and is a key complex in explaining the reactivity and structure of [Fe(L)('N_HS_4')] complexes. **6** contains an iron center which is surprisingly only five-coordinate. The structure and distances of chiral **6** closely resemble the [Fe('N_HS_4')] cores of low-spin [Fe(L)('N_HS_4')] complexes, whereas the paramagnetism and high reactivity of **6** are typical of high-spin [Fe(L)('N_HS_4')] complexes.

Keywords: Crystal structures; Iron complexes; Phosphine complexes; Azido complexes; Sulfur ligand complexes

1. Introduction

Iron centers in a coordination sphere of sulfur donors are characteristic features of the active sites of metal enzymes such as hydrogenases and nitrogenases [2], and the X-ray structural model of the FeMo cofactor of the FeMo protein of FeMo nitrogenase [3] supports the assumption that coordination and activation of the N_2 molecule in nitrogenases may take place at such centers.

In order to understand the high catalytic activity of these enzyme centers we have investigated complexes exhibiting sulfur coordinated iron centers *and* the ability to coordinate enzymatically relevant molecules. Recently we reported the coordination of intermediate and final products of N_2 fixation such as N_2H_2, N_2H_4 and NH_3 to the [Fe('N_HS_4')] fragment [4], however, N_2 as the starting molecule of N_2 fixation could not yet be coordinated.

The [Fe('N_HS_4')] fragment exists in the two diastereomeric forms I and II. Coordination of σ–π ligands (N_2H_2, PMe_3 or CO) leads to the chiral form I containing low-spin Fe(II) centers; coordination of σ ligands (N_2H_4

☆For Part CV see Ref. [1].

*Corresponding author.

SSDI 0020-1693(94)04017-P

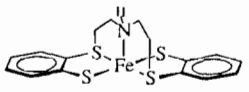

I

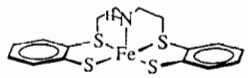

II

or NH_3) causes the achiral *meso* form II with high-spin Fe(II) centers [4]. Therefore, coordination of the σ–π ligand N_2 can only be expected if the [Fe('N_HS_4')] fragment has the chiral low-spin configuration I.

We tried to achieve coordination of N_2 to the [Fe('N_HS_4')] fragment by various ways: (i) substitution of phosphine ligands in labile [Fe(PR_3)('N_HS_4')] complexes containing the chiral low-spin fragment I, (ii) transformation of an azido into an N_2 ligand within the coordination sphere of the [Fe('N_HS_4')] fragment, (iii) deprotonation of the N_H donor of the 'N_HS_4' ligand of suitable precursors, (iv) direct reaction of N_2 with the particularly reactive complex [Fe('N_HS_4')]·THF.

2. Experimental

2.1. General

Unless otherwise noted all operations were carried out under nitrogen atmosphere at room temperature using Schlenk techniques. Solvents were dried and distilled before use. Spectra were recorded on the following instruments: IR: Perkin-Elmer 983 and Perkin-Elmer 1620 FT IR; mass spectra: Varian MAT 212; magnetic moments: Johnson Matthey susceptibility balance. [Fe('N_HS_4')]·THF (**6**) [4b], [Fe(MeOH)('N_HS_4')] [4b], PMe_3 [5], PMe_2Ph [6] and $PMePh_2$ [6] were prepared by literature methods; PBu_3 was purchased from Aldrich. NEt_4N_3 was obtained by reaction of NaN_3 and NEt_4Cl in MeOH and subsequent recrystallization from acetone.

2.2. X-ray structure determination of [Fe(PMe_3)('N_HS_4')] (1), [Fe(PMe_2Ph)('N_HS_4')] (2), [Fe(PBu_3)('N_HS_4')] (3), (NEt_4)[Fe(N_3)('N_HS_4')] (5) and [Fe('N_HS_4')]·THF (6)

Single crystals of [Fe(PMe_3)('N_HS_4')] (**1**) and [Fe(PMe_2Ph)('N_HS_4')] (**2**) were obtained by layering saturated THF solutions of the complexes with Et_2O to which a drop of the respective phosphine had been added. Single crystals of [Fe(PBu_3)('N_HS_4')] (**3**) grew when the Et_2O solution slowly evaporated. Single crystals of (NEt_4)[Fe(N_3)('N_HS_4')] (**5**) formed from a DMF solution layered with Et_2O, and single crystals of [Fe('N_HS_4')]·THF (**6**) were obtained from a saturated boiling THF solution upon cooling to room temperature. Suitable crystals were sealed in glass capillaries. The structures were solved by direct methods (SHELXTL-PLUS). Non-hydrogen atoms were refined with anisotropic and hydrogen atoms with common isotropic temperature factors. The positions of the hydrogen atoms in the structures of [Fe(PMe_3)('N_HS_4')] (**1**), [Fe(PMe_2Ph)('N_HS_4')] (**2**), [Fe(PBu_3)('N_HS_4')] (**3**) and [Fe('N_HS_4')]·THF (**6**) were taken from the difference Fourier syntheses and were refined as rigid groups. In (NEt_4)[Fe(N_3)('N_HS_4')] (**5**) the aromatic hydrogen atoms were calculated for ideal geometries and restricted during refinement. The hydrogen atoms of the amino, the methylene and the methyl groups were calculated for ideal tetrahedra and allowed to rotate around the central atom during refinement.

Table 1 contains selected crystallographic data and Table 2 gives the final atomic coordinates.

2.3. Syntheses and reactions

2.3.1. [Fe(PMe_3)('N_HS_4')] (1)

0.5 ml (4.83 mmol) of PMe_3 was added to a suspension of [Fe(MeOH)('N_HS_4')] (510 mg, 1.16 mmol) in 50 ml of THF. The resulting deep green solution was filtered after 1 h, evaporated to one half of its volume, and cooled to −20 °C. The precipitating greenish gray crystals were collected after 24 h and dried in vacuo. Yield 300 mg (53%).

Anal. Calc. for $C_{19}H_{26}FeNPS_4$ (483.5): C, 47.20; H, 5.42; N, 2.90. Found: C, 47.24; H, 5.50; N, 2.92%. IR (KBr, cm^{-1}): 3180 ν(NH), 938 δ(PCH). FD mass spectrum (THF, m/z): 407 [Fe('N_HS_4')]$^+$.

2.3.2. [Fe(PMe_2Ph)('N_HS_4')] (2)

0.6 ml (5.35 mmol) of PMe_2Ph was added to a suspension of [Fe(MeOH)('N_HS_4')] (470 mg, 1.07 mmol) in 50 ml of THF. The resulting deep green solution was filtered after 2 h, concentrated to one half of its volume and layered with 30 ml of Et_2O. The precipitating green crystals were collected after 2 days, washed with Et_2O and dried in vacuo. Yield 370 mg (63%).

Anal. Calc. for $C_{24}H_{28}FeNPS_4$ (545.6): C, 52.84; H, 5.17; N, 2.57; S, 23.51. Found: C, 52.82; H, 5.30; N, 2.63; S, 23.61%. IR (KBr, cm^{-1}): 3190 ν(NH), 933 δ(PCH). EI mass spectrum (*m/z*): 407 [Fe('N_HS_4')]$^+$.

2.3.3. [Fe(PBu_3)('N_HS_4')] (3)

A suspension of 655 mg (1.50 mmol) [Fe(MeOH)('N_HS_4')] in 50 ml of THF was combined with 1 ml (4 mmol) of PBu_3 and stirred for 2 h in the course of which a deep green solution developed. It was filtered and evaporated. The resulting viscous residue was redissolved in 20 ml of MeOH, the solution was filtered and reduced in volume to 5 ml. A green solid precipitated which was separated and dried in vacuo. Yield 525 mg (58%).

Anal. Calc. for $C_{28}H_{44}FeNPS_4$ (609.8): C, 55.16; H, 7.27; N, 2.30; S, 21.03. Found: C, 54.96; H, 7.45; N,

Table 1
Selected crystallographic data of [Fe(PMe$_3$)('N_HS_4')] (**1**), [Fe(PMe$_2$Ph)('N_HS_4')] (**2**), [Fe(PBu$_3$)('N_HS_4')] (**3**), (NEt$_4$)[Fe(N$_3$)('N_HS_4')] (**5**) and [Fe('N_HS_4')]·THF (**6**)

Compound	[Fe(PMe$_3$)('N_HS_4')] (**1**)	[Fe(PMe$_2$Ph)('N_HS_4')] (**2**)	[Fe(PBu$_3$)('N_HS_4')] (**3**)	(NEt$_4$)[Fe(N$_3$)('N_HS_4')] (**5**)	[Fe('N_HS_4')]·THF (**6**)
Formula	$C_{19}H_{26}NS_4FeP$	$C_{24}H_{28}NS_4FeP$	$C_{28}H_{44}NS_4FeP$	$C_{24}H_{37}N_5S_4Fe$	$C_{20}H_{25}NS_4FeO$
Molecular weight	483.5	545.5	609.8	597.7	479.5
Space group	$P\bar{1}$	$P2_1/c$	$P2_1/c$	$P2_1/n$	$P2_1/c$
Crystal system	triclinic	monoclinic	monoclinic	monoclinic	monoclinic
Cell dimensions					
a (pm)	929.5(3)	921.5(2)	919.3(2)	1254.5(4)	1619.0(4)
b (pm)	1047.6(3)	2276.2(6)	1466.8(6)	1107.2(4)	1196.7(3)
c (pm)	1186.9(3)	1196.7(2)	2313.7(6)	2018.6(6)	1224.2(4)
α (°)	69.39(9)				
β (°)	83.58(3)	99.83(1)	95.69(2)	90.93(2)	112.45(2)
γ (°)	83.80(3)				
V (pm^3)	$1071(1)\times10^6$	$2473(1)\times10^6$	$3103(2)\times10^6$	$2804(2)\times10^6$	$2192(1)\times10^6$
Z	2	4	4	4	4
D_{calc} (g/cm^3)	1.50	1.47	1.31	1.37	1.45
Temperature (K)	293	293	200	293	200
Diffractometer	Siemens P4	Siemens P4	Siemens P4	Siemens P4	Siemens P4
Radiation	Mo Kα	Mo Kα	Mo Kα	Mo Kα	Mo Kα
Scan technique	ω-scan	ω-scan	ω-scan	ω-scan	ω-scan
Scan speed (°/min)	3–29	3–29	3–29	3–29	3–29
$2\theta_{max}$ (°)	54	54	54	54	54
Reflexions measured	6186	5873	7215	7862	7688
Independent reflexions	4695	4413	6633	6161	4806
Observed reflexions	2988	2131	2475	1875	2704
σ Criterion	$F>4\sigma(F)$	$F>4\sigma(F)$	$F>4\sigma(F)$	$F>4\sigma(F)$	$F>4\sigma(F)$
Parameters refined	235	280	316	308	244
R/R_w	0.048/0.043	0.045/0.038	0.048/0.042	0.068/0.055	0.043/0.038

Table 2
Atomic coordinates ($\times 10^4$) and isotropic thermal parameters ($pm^2 \times 10^{-1}$)

	x	y	z	U_{eq}[a]
[Fe(PMe$_3$)('N$_H$S$_4$')] (**1**)				
Fe(1)	2272(1)	74(1)	7244(1)	30(1)
S(1)	2187(2)	1719(1)	8136(1)	36(1)
S(2)	4266(2)	922(1)	6119(1)	33(1)
S(3)	103(2)	−539(2)	8168(1)	37(1)
S(4)	2274(2)	−1562(2)	6356(1)	41(1)
P(1)	3453(2)	−1335(2)	8779(1)	34(1)
C(1)	3964(8)	−3090(6)	8865(6)	59(3)
C(2)	5243(6)	−842(6)	8902(6)	51(3)
C(3)	2523(7)	−1589(6)	10285(5)	52(3)
C(15)	4652(6)	2288(5)	6587(5)	34(2)
C(14)	5895(6)	2988(6)	6051(6)	41(2)
C(13)	6227(7)	4033(6)	6415(6)	48(3)
C(12)	5332(8)	4369(6)	7289(6)	52(3)
C(11)	4092(7)	3687(6)	7821(6)	42(2)
C(10)	3727(6)	2614(5)	7465(5)	34(2)
C(25)	−40(7)	−2189(6)	8066(6)	43(2)
C(24)	−1110(7)	−3003(7)	8816(6)	57(3)
C(23)	−1191(8)	−4295(7)	8743(7)	71(4)
C(22)	−244(8)	−4747(6)	7980(7)	62(3)
C(21)	824(7)	−3924(6)	7235(6)	48(3)
C(20)	910(7)	−2600(6)	7264(5)	43(2)
N(1)	1136(5)	1381(5)	5830(4)	36(2)
C(16)	3450(7)	1950(6)	4716(5)	46(3)
C(17)	1957(7)	2522(6)	5014(5)	46(2)
C(26)	−1099(6)	539(6)	7001(6)	46(3)
C(27)	−339(6)	1812(6)	6235(6)	45(2)
[Fe(PMe$_2$Ph)('N$_H$S$_4$')] (**2**)				
Fe(1)	1150(1)	6481(1)	3310(1)	43(1)
P(1)	2796(2)	6020(1)	2471(2)	45(1)
C(35)	1706(9)	4899(4)	1767(6)	59(4)
C(34)	1638(10)	4290(4)	1834(8)	76(4)
C(33)	2627(12)	3999(3)	2631(9)	80(5)
C(32)	3665(10)	4286(4)	3369(7)	75(4)
C(31)	3733(9)	4891(4)	3349(6)	63(4)
C(30)	2764(9)	5201(3)	2530(6)	49(3)
C(40)	2699(8)	6156(3)	965(5)	67(3)
C(50)	4739(8)	6178(3)	2955(6)	69(4)
S(1)	−602(2)	6387(1)	1698(2)	65(1)
S(2)	211(2)	5685(1)	4001(1)	51(1)
S(3)	1853(3)	7346(1)	2748(2)	66(1)
S(4)	2803(2)	6575(1)	4972(1)	50(1)
C(15)	−1168(8)	5397(4)	2896(6)	55(3)
C(14)	−1879(10)	4880(4)	3061(7)	71(4)
C(13)	−2943(11)	4653(4)	2225(9)	86(5)
C(12)	−3242(10)	4956(5)	1231(8)	83(5)
C(11)	−2599(10)	5475(4)	1029(7)	68(4)
C(10)	−1528(9)	5720(3)	1891(7)	60(3)
C(25)	3436(9)	7542(3)	3763(6)	54(3)
C(24)	4299(11)	8018(4)	3568(7)	74(4)
C(23)	5493(11)	8174(4)	4341(9)	87(5)
C(22)	5840(10)	7863(4)	5330(8)	78(4)
C(21)	5020(9)	7382(3)	5530(6)	59(4)
C(20)	3804(9)	7208(3)	4756(6)	48(3)
C(16)	−1033(9)	6029(4)	4865(6)	77(4)
C(17)	−1097(16)	6617(5)	4737(12)	225(10)
N(1)	−359(7)	6948(3)	4100(5)	67(3)
C(26)	450(11)	7815(4)	3236(8)	101(5)
C(27)	−278(19)	7522(5)	3967(14)	292(14)

(*continued*)

Table 2 (*continued*)

	x	y	z	U_{eq}[a]
[Fe(PBu$_3$)('N$_H$S$_4$')] (**3**)				
Fe(1)	5434(2)	3414(1)	8930(1)	27(1)
S(1)	7143(3)	4284(2)	9486(1)	34(1)
S(2)	5416(3)	4483(2)	8243(1)	35(1)
S(3)	5183(3)	2484(2)	9668(1)	29(1)
S(4)	3640(3)	2612(2)	8374(1)	31(1)
C(15)	6999(12)	5176(7)	8408(4)	38(4)
C(14)	7430(15)	5805(8)	8022(5)	54(5)
C(13)	8626(16)	6324(9)	8160(5)	65(6)
C(12)	9411(13)	6241(8)	8685(5)	55(5)
C(11)	9001(12)	5603(8)	9104(4)	45(4)
C(10)	7725(12)	5060(7)	8970(4)	36(4)
C(25)	3979(10)	1609(7)	9372(4)	28(3)
C(24)	3729(11)	852(8)	9725(4)	34(4)
C(23)	2738(12)	179(7)	9513(4)	42(4)
C(22)	2041(11)	275(8)	8962(4)	40(4)
C(21)	2293(11)	1010(7)	8612(4)	35(4)
C(20)	3277(10)	1700(7)	8809(3)	29(3)
N(1)	3826(8)	4202(6)	9249(3)	30(3)
C(16)	4031(13)	5281(7)	8454(4)	45(4)
C(17)	2990(12)	4732(8)	8796(4)	44(4)
C(26)	3897(11)	3165(7)	10061(4)	35(4)
C(27)	2921(11)	3683(7)	9619(4)	39(4)
P(1)	7193(3)	2561(2)	8582(1)	29(1)
C(31)	7770(11)	2919(7)	7867(4)	33(4)
C(32)	6641(12)	2770(7)	7367(3)	40(4)
C(33)	7076(14)	3181(10)	6826(4)	71(6)
C(34)	6007(17)	3023(9)	6315(5)	84(7)
C(41)	6787(11)	1351(7)	8455(4)	34(4)
C(42)	7913(12)	735(8)	8214(4)	42(4)
C(43)	7449(13)	−229(8)	8129(4)	54(5)
C(44)	8526(16)	−833(9)	7867(5)	76(6)
C(51)	8987(9)	2511(8)	9012(3)	32(3)
C(52)	8977(10)	1991(8)	9582(4)	39(4)
C(53)	10360(11)	2096(7)	9981(4)	40(4)
C(54)	10410(11)	1522(8)	10534(4)	51(4)
(NEt$_4$)[Fe(N$_3$)('N$_H$S$_4$')] (**5**)				
Fe(1)	6471(1)	7539(2)	107(1)	41(1)
N(1)	4800(7)	8086(8)	−242(4)	43(4)
N(2)	7535(9)	6300(11)	564(6)	57(5)
N(3)	7690(9)	5297(13)	485(5)	49(5)
N(4)	7867(10)	4269(12)	411(6)	70(5)
S(1)	6874(3)	9417(3)	678(2)	53(1)
S(2)	5374(3)	7189(3)	1203(2)	52(1)
S(3)	5924(3)	5713(3)	−667(1)	43(1)
S(4)	7392(3)	8206(3)	−852(2)	58(1)
C(15)	6106(10)	8155(13)	1764(6)	52(5)
C(14)	6056(11)	7876(13)	2436(6)	67(6)
C(13)	6620(12)	8579(16)	2879(7)	79(8)
C(12)	7182(11)	9566(15)	2673(8)	79(8)
C(11)	7237(10)	9828(13)	2012(8)	67(6)
C(10)	6723(11)	9120(12)	1542(6)	51(5)
C(25)	6762(9)	5927(11)	−1368(5)	37(5)
C(24)	6805(9)	4995(12)	−1828(6)	50(5)
C(23)	7534(11)	5080(13)	−2341(6)	56(6)
C(22)	8204(10)	6068(13)	−2379(6)	54(6)
C(21)	8156(10)	7008(12)	−1937(6)	54(6)
C(20)	7395(10)	6963(11)	−1416(5)	40(5)
C(16)	4258(9)	8169(11)	924(5)	54(5)
C(17)	3919(9)	7837(11)	227(5)	49(5)
C(26)	4641(9)	6250(11)	−970(5)	44(5)

(*continued*)

Table 2 (*continued*)

	x	y	z	U_{eq}[a]
C(27)	4538(9)	7619(13)	−922(5)	56(5)
N(5)	9748(9)	2335(11)	−1151(5)	57(4)
C(1)	9007(11)	3360(14)	−1093(7)	83(7)
C(2)	9514(11)	4587(11)	−929(6)	72(6)
C(3)	10649(10)	2566(15)	−1616(6)	85(6)
C(4)	10216(12)	2897(14)	−2327(6)	113(9)
C(5)	9110(11)	1204(14)	−1362(8)	90(8)
C(6)	9824(12)	118(12)	−1548(8)	96(8)
C(7)	10315(11)	2061(14)	−489(7)	86(7)
C(8)	9558(11)	1798(13)	93(7)	91(7)
[Fe('N_HS_4')]·THF (**6**)				
Fe(1)	10042(1)	9330(1)	7696(1)	31(1)
S(1)	9053(1)	9509(1)	8629(1)	38(1)
S(2)	8680(1)	9573(1)	5761(1)	41(1)
S(3)	11456(1)	8675(1)	9323(1)	37(1)
S(4)	10891(1)	10753(1)	7386(1)	34(1)
C(15)	7809(3)	9382(4)	6297(5)	39(2)
C(14)	6937(4)	9262(5)	5452(6)	56(3)
C(13)	6239(4)	9109(6)	5849(7)	67(3)
C(12)	6413(5)	9084(6)	7044(7)	68(4)
C(11)	7271(4)	9197(5)	7863(6)	50(3)
C(10)	7992(3)	9358(4)	7505(5)	36(2)
C(25)	12253(3)	9619(4)	9172(5)	34(2)
C(24)	13144(4)	9460(5)	9899(5)	42(2)
C(23)	13808(3)	10191(5)	9863(5)	49(3)
C(22)	13558(4)	11063(5)	9092(6)	52(3)
C(21)	12671(4)	11236(4)	8360(6)	47(3)
C(20)	11999(3)	10522(4)	8374(4)	31(2)
N(1)	10228(3)	7870(3)	6803(4)	36(2)
C(16)	8801(4)	8191(5)	5169(5)	43(2)
C(17)	9786(4)	7967(5)	5503(5)	46(3)
C(26)	11596(4)	7463(4)	8502(6)	48(3)
C(27)	11197(4)	7622(5)	7180(5)	41(3)
O(30)	4569(3)	7488(4)	6657(4)	66(2)
C(31)	4734(5)	7020(7)	7759(7)	80(4)
C(32)	4031(7)	7388(8)	8147(8)	106(6)
C(33)	3453(6)	8136(9)	7223(8)	100(5)
C(34)	3995(5)	8402(6)	6570(7)	74(4)

[a]Equivalent isotropic U defined as one third of the trace of the orthogonalized U_{ij} tensor.

2.28; S, 20.90%. IR (KBr, cm^{-1}): 3180 ν(NH), 934 δ(PCH). EI mass spectrum (*m/z*): 407 [Fe('N_HS_4')]$^+$.

2.3.4. *[Fe(PMePh$_2$)('N_HS_4')] (4)*

1 ml (5.0 mmol) of $PMePh_2$ was added to a suspension of [Fe(MeOH)('N_HS_4')] (440 mg, 1.0 mmol) in 50 ml of THF. The resulting light green solution was filtered over filter pulp, reduced in volume to one half and layered with 25 ml of hexane. The precipitating green needles were collected after 12 h, washed with hexane and dried in vacuo. Yield 320 mg (53%).

Anal. Calc. for $C_{29}H_{30}FeNPS_4$ (607.6): C, 57.32; H, 4.98; N, 2.31; S, 21.11. Found: C, 57.52; H, 5.02; N, 2.32; S, 21.21%. IR (KBr, cm^{-1}): 3190 ν(NH), 941 δ(PCH). EI mass spectrum (*m/z*): 407 [Fe('N_HS_4')]$^+$.

2.3.5. *[Fe(CO)('N_HS_4')] from [Fe(PR$_3$)('N_HS_4')] and CO*

CO was bubbled through solutions of the respective [Fe(PR_3)('N_HS_4')] complexes (0.5 mmol in 20 ml of THF). The colour of the solutions immediately changed from green to red, and in the IR spectra the ν(CO) absorption of [Fe(CO)('N_HS_4')] at 1960 cm^{-1} reached its maximum intensity after 10–15 s.

2.3.6. *(NEt$_4$)[Fe(N$_3$)('N_HS_4')] (5)*

1.30 g (7.5 mmol) of NEt_4N_3 were added to a stirred yellowish green solution of [Fe(MeOH)('N_HS_4')] (1.10 g, 2.5 mmol) in 50 ml of DMF. The mixture was evaporated to dryness after 2 h, and the resulting brown residue was washed three times with 50 ml of acetone yielding a yellow powder which was dried in vacuo. Yield 1 g (71%).

Anal. Calc. for $C_{24}H_{37}FeN_5S_4$ (579.7): C, 49.73; H, 6.43; N, 12.08. Found: C, 50.24; H, 6.81; N, 12.06%. IR (KBr, cm^{-1}): 3240 ν(NH), 2049 ν(N_3). EI mass spectrum (*m/z*): 450 [Fe(N_3)('N_HS_4')]$^+$.

2.3.7. *Deprotonation of [Fe(CO)('N_HS_4')] with n-BuLi*

0.65 ml (1.0 mmol) of n-BuLi was added dropwise to 435 mg (1.0 mmol) of [Fe(CO)('N_HS_4')] in 40 ml of THF at −78 °C. The mixture was stirred for 1 h at −78 °C and then slowly warmed up to room temperature in the course of which its color changed from red to green. Simultaneously, the ν(CO) IR absorption of [Fe(CO)('N_HS_4')] at 1960 cm^{-1} disappeared and a new ν(CO) band at 1940 cm^{-1} indicated the formation of Li[Fe(CO)('NS_4')].

2.3.8. *[Fe(CO)('$N_{Me}S_4$')]*

A THF solution containing 1.0 mmol of Li[Fe(CO)('NS_4')] which had been obtained by the preceding method was combined with 0.1 ml (1.6 mmol) of MeI at −78 °C, whereupon the color immediately changed from green to red. The mixture was warmed to room temperature and evaporated to dryness. The resulting black–red residue was washed with MeOH and recrystallized from a saturated CH_2Cl_2 solution layered with Et_2O. Yield 95 mg (21%).

Anal. Calc. for $C_{18}H_{19}FeNOS_4$ (449.5): C, 48.10; H, 4.26; N, 3.12. Found: C, 48.06; H, 4.26; N, 2.88%. IR (KBr, cm^{-1}): 1937 ν(CO). NMR (CD_2Cl_2, δ (ppm)): ^{1}H NMR (270 MHz): 7.6–6.8 (m, 8H, C_6H_4), 3.9–2.3 (m, 8H, C_2H_4), 2.8 (s, 3H, CH_3); $^{13}C\{^1H\}$ NMR (67.94 MHz): 218 (*C*O), 158, 134, 132, 130, 129, 122 (C_6H_4), 60, 43 (C_2H_4), 50 (CH_3). FD mass spectrum (THF, *m/z*): 449 [Fe(CO)('$N_{Me}S_4$')]$^+$.

3. Results and discussion

3.1. *[Fe(PR$_3$)('N_HS_4')] complexes*

The diamagnetic PMe_3 complex [Fe(PMe_3)('N_HS_4')] (**1**) which we described recently, contains, according

to its ^{13}C NMR spectrum, the [Fe('N_HS_4')] core in the chiral form I. **1** was initially obtained from [Fe(CO)('N_HS_4')] and PMe_3 by thermal substitution of CO [7], and proved inert towards substitution of PMe_3 by N_2. Anticipating that bulkier phosphines, due to their larger cone angles, are bound more labile to the Fe center so that they can be substituted more easily, we synthesized and investigated [Fe(PR_3)('N_HS_4')] complexes with sterically demanding PR_3 ligands.

The phosphine complexes formed according to Eq. (1). **1–4** were isolated as green crystals and are well

$$[Fe(MeOH)('N_HS_4')] + L_{exc.} \xrightarrow[-MeOH]{THF} [Fe(L)('N_HS_4')] \quad (1)$$

L = PMe_3 (**1**), PMe_2Ph (**2**), PBu_3 (**3**), $PMePh_2$ (**4**)

soluble in THF, CH_2Cl_2 and acetone. Their KBr IR spectra show intense δ(PCH) absorptions of the PR_3 ligands. As expected, **2–4** proved more labile than **1**. In fact, they dissociate so rapidly in solution that no ^1H NMR spectra could be obtained, and single crystals only formed from solutions to which an excess of the respective phosphine had been added. The even bulkier phosphines PPh_3 and PCy_3 could not be coordinated to the [Fe('N_HS_4')] fragment.

In order to elucidate and possibly confirm the assumed structural reasons for the lability of the phosphine ligands, **2** and **3**, and, for the sake of comparison, also **1**, were characterized by X-ray structure analyses.

3.2. X-ray structure analyses and molecular properties of 1, 2 and 3

Fig. 1 shows the molecular structures of **1**, **2** and **3**. Table 3 lists selected distances and angles.

In all three complexes, the iron centers are surrounded pseudo-octahedrally by one phosphorus, one nitrogen and four sulfur donors. The [Fe('N_HS_4')] cores possess C_1 symmetry and the chiral configuration I in which thioether and thiolate sulfur donors assume *trans* positions and approximately form a plane. Amine donors and phosphine coligands are *trans* to each other. Bond lengths and angles of the [Fe('N_HS_4')] cores show no distinct trend in **1**, **2** and **3** and are in the range which is observed for low-spin [Fe(L)('N_HS_4')] complexes. In contrast, the Fe–P distances vary significantly and can be correlated to the phosphine cone angles. Table 4 shows that complex **3** having the phosphine with the largest cone angle also exhibits the largest Fe–P distance. Thus, it can be understood why $PMePh_2$ (cone angle 136°) still forms highly labile [Fe($PMePh_2$)('N_HS_4')] (**4**), but PPh_3 and PCy_3 with their markedly larger cone angles of 145 and 170° do not coordinate to the [Fe('N_HS_4')] fragment.

3.3. Reactions of the phosphine complexes

All [Fe(PR_3)('N_HS_4')] complexes described here reacted rapidly with CO. Bubbling CO through solutions of the green phosphine complexes immediately yielded the deep red [Fe(CO)('N_HS_4')] which was identified by

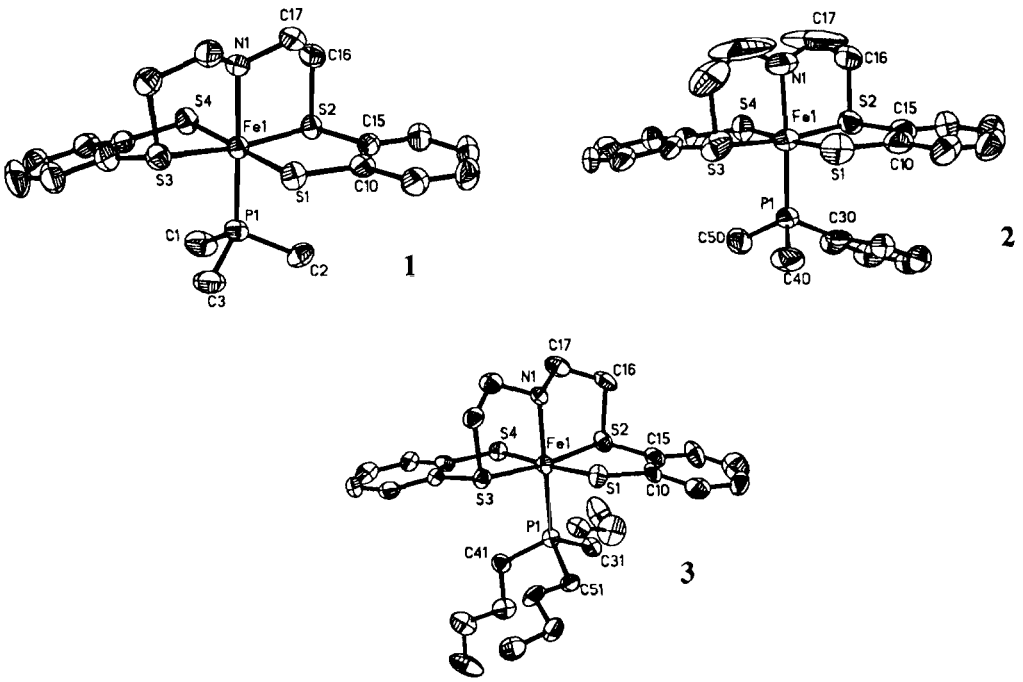

Fig. 1. Molecular structures of [Fe(PMe_3)('N_HS_4')] (**1**), [Fe(PMe_2Ph)('N_HS_4')] (**2**) and [Fe(PBu_3)('N_HS_4')] (**3**) (H atoms omited).

Table 3
Selected distances (pm) and angles (°) of [Fe(PMe_3)('N_HS_4')] (**1**), [Fe(PMe_2Ph)('N_HS_4')] (**2**) and [Fe(PBu_3)('N_HS_4')] (**3**)

[Fe(PMe_3)('N_HS_4')] (**1**)			
Fe(1)–S(1)	230.9(2)	S(1)–Fe(1)–S(2)	89.3(1)
Fe(1)–S(2)	223.1(2)	S(2)–Fe(1)–S(3)	171.8(1)
Fe(1)–S(3)	222.9(2)	S(1)–Fe(1)–S(4)	178.1(1)
Fe(1)–S(4)	230.7(2)	S(2)–Fe(1)–S(4)	92.2(1)
Fe(1)–P(1)	221.5(2)	S(1)–Fe(1)–P(1)	87.9(1)
Fe(1)–N(1)	206.7(4)	S(2)–Fe(1)–P(1)	94.9(1)
S(1)–C(10)	175.3(6)	S(1)–Fe(1)–N(1)	91.9(2)
S(2)–C(15)	178.8(7)	S(2)–Fe(1)–N(1)	86.1(1)
S(2)–C(16)	183.2(6)	P(1)–Fe(1)–N(1)	179.0(1)
N(1)–C(17)	147.1(7)	Fe(1)–P(1)–C(1)	119.9(2)
[Fe(PMe_2Ph)('N_HS_4')] (**2**)			
Fe(1)–P(1)	222.1(2)	P(1)–Fe(1)–S(1)	90.7(1)
Fe(1)–S(1)	230.4(2)	P(1)–Fe(1)–S(2)	97.0(1)
Fe(1)–S(2)	222.8(2)	S(1)–Fe(1)–S(2)	88.5(1)
Fe(1)–S(3)	221.1(2)	S(2)–Fe(1)–S(3)	171.6(1)
Fe(1)–S(4)	229.9(2)	S(1)–Fe(1)–S(4)	177.1(1)
Fe(1)–N(1)	209.8(7)	S(2)–Fe(1)–S(4)	89.8(1)
S(1)–C(10)	177.5(8)	P(1)–Fe(1)–N(1)	177.8(2)
S(2)–C(15)	179.4(7)	S(1)–Fe(1)–N(1)	90.1(2)
S(2)–C(16)	184.4(9)	S(2)–Fe(1)–N(1)	85.1(2)
C(17)–N(1)	133.7(16)	Fe(1)–P(1)–C(30)	116.0(3)
[Fe(PBu_3)('N_HS_4')] (**3**)			
Fe(1)–S(1)	231.4(3)	S(1)–Fe(1)–S(2)	88.0(1)
Fe(1)–S(2)	223.2(3)	S(2)–Fe(1)–S(3)	171.0(1)
Fe(1)–S(3)	221.5(3)	S(1)–Fe(1)–S(4)	176.8(1)
Fe(1)–S(4)	231.0(3)	S(2)–Fe(1)–S(4)	90.4(1)
Fe(1)–N(1)	207.0(8)	S(1)–Fe(1)–N(1)	87.8(2)
Fe(1)–P(1)	225.5(3)	S(2)–Fe(1)–N(1)	84.6(2)
S(1)–C(10)	177.2(10)	S(1)–Fe(1)–P(1)	91.9(1)
S(2)–C(15)	178.4(11)	S(2)–Fe(1)–P(1)	95.2(1)
S(2)–C(16)	183.1(12)	N(1)–Fe(1)–P(1)	179.7(3)
N(1)–C(17)	146.2(12)	Fe(1)–P(1)–C(31)	116.0(3)

Table 4
Comparison of iron–donor distances (pm) and phosphine cone angles (°) [8] in [Fe(PR_3)('N_HS_4')] complexes **1**, **2** and **3**

PR_3	PMe_3	PMe_2Ph	PBu_3
Cone angle	118	122	132
d(Fe–P)	221.5(2)	222.1(2)	225.5(3)
d(Fe–N)	206.7(4)	209.8(7)	207.0(8)
$\bar{d}$(Fe–thiolate-S)	230.8(2)	230.2(2)	231.2(3)
$\bar{d}$(Fe–thioether-S)	223.0(2)	222.0(2)	222.4(3)

its intense ν(CO) IR absorption at 1960 cm^{-1} (Eq. (2)).

$$[Fe(L)('N_HS_4')] + CO \xrightarrow[-L]{THF} [Fe(CO)('N_HS_4')] \quad (2)$$

L = PMe_3 (**1**), PMe_2Ph (**2**), PBu_3 (**3**), $PMePh_2$ (**4**)

In contrast to our expectations, even the PMe_3 complex **1**, the NMR spectrum of which did not indicate any dissociation of the PMe_3 ligand, exchanged its phosphine ligand for CO as rapidly as the other PR_3 complexes. Mechanistically, it can be assumed that the exchange takes place in all complexes via dissociation of the iron–phosphine bond yielding [Fe('N_HS_4')] fragments. They can be expected to exist at least initially in the chiral low-spin configuration I favoring the coordination not only of CO but also the σ–π ligand N_2. All attempts, however, to react the phosphine complexes with N_2 have been unsuccessful so far. Even under 150 bar of N_2, no coordination of N_2 to the [Fe('N_HS_4')] fragment could be observed.

3.4. Synthesis, structure and reactivity of (NEt$_4$)[Fe(N$_3$)('N$_H$S$_4$')] (5)

In several cases, syntheses of N_2 complexes could be achieved by oxidative transformation of an azido ligand into an N_2 ligand. Examples are [cpMn$(CO)_2N_2$], $[Ru(das)_2Cl(N_2)]^+$ (das = *o*-phenylenbis(dimethylarsine)) or $[Ru(NH_3)_5N_2]^{2+}$ [9]. For this reason, the [Fe$(N_3)('N_HS_4')]^-$ anion was one of our target complexes. It formed as the yellow NEt_4^+ salt (NEt_4)[Fe$(N_3)('N_HS_4')$] (**5**) according to Eq. (3).

$$[Fe(MeOH('N_HS_4')] + NEt_4N_3 \xrightarrow[-MeOH]{DMF} (NEt_4)[Fe(N_3)('N_HS_4')] \quad (3)$$

5

5 shows an intense and characteristic $\nu(N_3)$ absorption at 2050 cm^{-1} in its KBr IR spectrum. The magnetism (μ_{eff} = 5.05 BM, 297 K) corresponds to a high-spin Fe(II) center with four unpaired electrons and prevented the recording of high resolution NMR spectra. **5** is well soluble in DMF, in which, however, partial decoordination of the azido ligand takes place. This was concluded from the IR spectra of such DMF solutions showing the $\nu(N_3)$ band of **5** at 2050 cm^{-1} and an additional absorption at 2000 cm^{-1} which could be assigned to free azido ions by comparison with DMF solutions of NEt_4N_3. Decoordination of the azido ligand was diminished, but not completely prevented in less polar solvents such as CH_2Cl_2, in which, however, **5** is only slightly soluble.

Paramagnetism and lability of the azido complex indicated that the azido ligand functions as a σ donor and the [Fe('N_HS_4')] fragment of **5** possesses the achiral configuration II. This was confirmed by X-ray structure

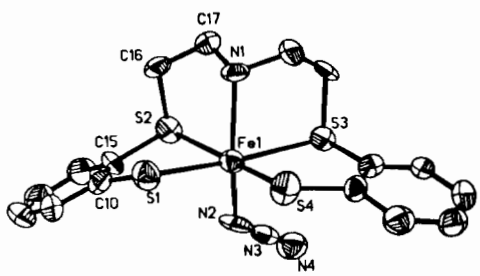

Fig. 2. Molecular structure of the anion of (NEt_4)[Fe$(N_3)('N_HS_4')$] (**5**) (H atoms omitted).

Table 5
Selected distances (pm) and angles (°) of $(NEt_4)[Fe(N_3)('N_HS_4')]$ (**5**)

Fe(1)–N(1)	228.3(9)	N(1)–Fe(1)–N(2)	151.2(4)
Fe(1)–N(2)	211.4(12)	N(1)–Fe(1)–S(1)	95.8(2)
Fe(1)–S(1)	242.7(4)	N(2)–Fe(1)–S(1)	103.0(3)
Fe(1)–S(2)	265.2(4)	N(1)–Fe(1)–S(2)	79.0(2)
Fe(1)–S(3)	263.9(4)	N(2)–Fe(1)–S(2)	82.8(3)
Fe(1)–S(4)	238.7(4)	S(1)–Fe(1)–S(2)	80.6(1)
N(1)–C(17)	149.3(14)	N(1)–Fe(1)–S(3)	78.0(2)
N(2)–N(3)	113.9(18)	S(2)–Fe(1)–S(3)	104.4(1)
N(3)–N(4)	116.9(19)	N(1)–Fe(1)–S(4)	97.0(2)
S(1)–C(10)	178.8(13)	S(1)–Fe(1)–S(4)	91.1(1)
S(2)–C(15)	179.9(13)	S(2)–Fe(1)–S(4)	170.3(1)
S(2)–C(16)	185.2(12)	Fe(1)–N(2)–N(3)	132.8(10)

analysis. Fig. 2 shows the molecular structure and Table 5 lists selected distances and angles of **5**.

5 consists of discrete cations and anions. Two N and four S donors pseudo-octahedrally surround the iron center of the anion, and the sulfur donors approximately form a plane. As in all other high-spin $[Fe(L)('N_HS_4')]$ complexes, the thioether sulfur donors in **5** occupy *cis* positions. The iron–donor distances are markedly longer than in low-spin $[Fe(L)('N_HS_4')]$ complexes such as in the phosphine complexes described above. This is due to two electrons occupying antibonding σ^* molecular orbitals [4b].

The average Fe–S(thiolate), Fe–S(thioether) and Fe–N distances in the $[Fe('N_HS_4')]$ core of 240.7, 264.6 and 228.3 pm are not significantly longer compared with the distances in other high-spin $[Fe(L)('N_HS_4')]$ complexes [4b]. It is noted, however, that the Fe–L bond of **5** is only 211.4 pm long and thus distinctly shorter than in $[Fe(NH_3)('N_HS_4')]$ (218.9 pm) and $[Fe(N_2H_4)('N_HS_4')]$ (219.2 pm) which also contain nitrogen compounds acting as σ coligands [4b]. The azido ligand is practically linear, the bent Fe–N_3 angle is typical of azido complexes [10]. With standard deviations taken into account, the N–N distances within the azido ligand are approximately identical and indicate that the ionic character of the N_3^- ion stays largely conserved in the N_3 ligand. This result is consistent with the chemical behavior of **5**, in particular with the casy decoordination of the azido ligand in polar solvents.

Our major reason for the synthesis of **5** had been the wish to use it as a starting complex for the synthesis of the corresponding N_2 complex. However, the respective attempts remained unsuccessful. Neither heating **5** up to temperatures above 150 °C, nor oxidations of **5** by O_2, H_2O_2, I_2, *m*-chloroperbenzoic acid, chinon, $Pbac_4$ or PbO_2 even under drastic conditions led to the formation of N_2 complexes. Treatment of **5** with $NOBF_4$ in CH_2Cl_2 at −78 °C yielded, in addition to N_2O ($\nu(N_2O)$ 2220 cm^{-1}), $[Fe(NO)('N_HS_4')]BF_4$ which was characterized by its ν(NO) IR band at 1880 cm^{-1}.

3.5. Deprotonation of $[Fe(CO)('N_HS_4')]$

The amine N_H group of the 'N_HS_4' ligand in $[Fe(CO)('N_HS_4')]$ is suited for Brönsted acid–base reactions. Deprotonation of the amine σ donor could give an amido donor which, due to its σ–π donor properties, might function as a four-electron donor. Such a donor may strengthen the bonds to *trans* ligands, if they have empty π acceptor orbitals [11], however, it could also favor decoordination of these *trans* ligands because the resulting coordinatively unsaturated complex fragments are stabilized by π donation from the σ–π donor [12]. In the second case, deprotonation of $[Fe(CO)('N_HS_4')]$ could lead to $[Fe(CO)('NS_4')]^-$, which subsequently decoordinates CO in order to give $[Fe('NS_4')]^-$. This species can be expected to have the chiral low spin configuration I being favorable for the coordination of N_2.

Respective experiments indicated that $[Fe(CO)('N_HS_4')]$ only reactcd with strong bases like $LiN(SiMe_3)_2$ or n-BuLi. When the reaction according to Eq. (4) was carried out, IR monitoring showed that the ν(CO)

$$[Fe(CO)('N_HS_4')] + \text{n-BuLi} \xrightarrow[-\text{BuH}]{-78 \text{ to } +20\ ^\circ\text{C, THF}}$$

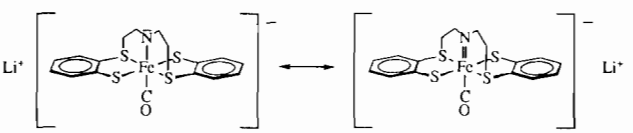

(4)

band of $[Fe(CO)('N_HS_4')]$ at 1960 cm^{-1} completely disappeared and a new ν(CO) band at 1940 cm^{-1} emerged (Fig. 3). It was assigned to the $[Fe(CO)('NS_4')]^-$ anion of which two schematic structures are shown in Eq. (4) indicating the σ donor or σ–π donor capability of the amido ligand.

This result proves that deprotonation of $[Fe(CO)('N_HS_4')]$ does not cause decoordination of the CO ligand, it rather suggests that, according to the decrease of the ν(CO) frequency, the Fe–CO bond was strengthened in the above discussed way instead.

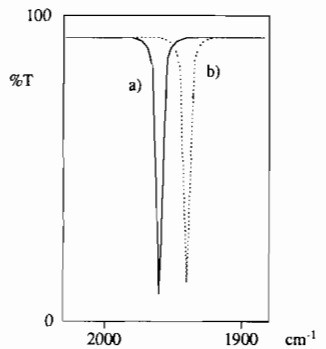

Fig. 3. ν(CO) IR spectra of (a) $[Fe(CO)('N_HS_4')]$ in THF, (b) after addition of n-BuLi at −78 °C and warming up to room temperature.

It was not possible to cleave off the CO ligand from $[Fe(CO)('NS_4')]^-$ by irradiating the reaction mixture with a UV lamp at −30 °C. When the reaction mixture was warmed up to room temperature, the starting complex $[Fe(CO)('N_HS_4')]$ regenerated within 2 h. This is traced back to deprotonation of the solvent THF by $[Fe(CO)('NS_4')]^-$, which must be an extremely strong Brönsted base.

Formation of $[Fe(CO)('NS_4')]^-$ in the reaction according to Eq. (4) was finally proved by its subsequent reaction with CH_3I according to Eq. (5). $[Fe(CO)-$

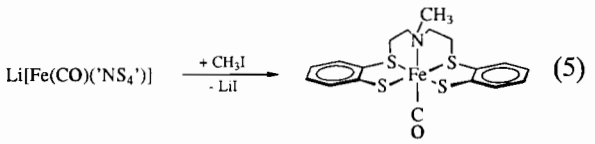

(5)

$('N_{Me}S_4')]$ having a methylated amine donor formed in low yields of about 25% consistent with previous results [7]. According to its ^{13}C NMR spectrum, $[Fe(CO)('N_{Me}S_4')]$ contains the achiral *meso* $[Fe('NS_4')]$ core in contrast to the chiral configuration of $[Fe(CO)('N_HS_4')]$. Obviously, a configurational rearrangement occurs when $[Fe(CO)('N_HS_4')]$ is converted into $[Fe(CO)('N_{Me}S_4')]$. This might require the intermediate formation of coordinatively unsaturated species with five-coordinate iron centers. As shown above, this cannot be achieved by decoordination of CO, but rather by decoordination of an S donor. With regard to the *meso* configuration of $[Fe(CO)('N_{Me}S_4')]$, we recently reported that steric reasons enforce the achiral *meso* configuration for all $[Fe(L)('N_RS_4')]$ complexes with R = alkyl [13].

3.6. X-ray structure determination and structural properties of $[Fe('N_HS_4')]\cdot THF$ (6)

The so far unsuccessful experiments to coordinate N_2 to the $[Fe('N_HS_4')]$ fragment via phosphine, azido and anionic carbonyl complexes led us to the reinvestigation of the highly reactive THF complex $[Fe('N_HS_4')]\cdot THF$ (**6**), that was not yet structurally characterized. **6** exhibits the same paramagnetism (μ_{eff} = 4.92, 293 K) as all other high-spin $[Fe(L)('N_HS_4')]$ complexes containing hard σ ligands L. Accordingly, **6** was assumed to have an analogous structure with a six-coordinate iron center and an achiral *meso* $[Fe('N_HS_4')]$ core. Coordination of N_2 to **6** was attempted under various conditions under standard or high pressure (150 bar), at temperatures ranging from −78 to +100 °C, in neutral medium and also in the presence of equivalent amounts of n-BuLi. In the latter case, we tried to induce the formation of the chiral low-spin configuration of the $[Fe('N_HS_4')]$ core by deprotonation of the N_H amine donor. In no case could coordination of N_2 to the $[Fe('N_HS_4')]$ fragment be observed, however, single crystals of $[Fe('N_HS_4')]\cdot THF$ (**6**) were obtained, first from solutions which contained n-BuLi and later also from neutral solutions. The single crystals, which had been obtained from these different sources, were characterized by X-ray structure analysis. They unexpectedly proved to be identical, and even more astonishing, to contain the THF molecule not as a ligand but as crystal solvate so that the iron center is only five-coordinate. Fig. 4 shows the molecular structure of $[Fe('N_HS_4')]\cdot THF$ (**6**) obtained from neutral THF solutions. Table 6 lists selected distances and angles.

In contrast to the solvent complex $[Fe(MeOH)-('N_HS_4')]$ [4b], the solvent molecule in $[Fe('N_HS_4')]\cdot THF$ (**6**) is not coordinated to the iron center, which is exclusively surrounded by the amine and the four sulfur donors of the 'N_HS_4' ligand. The resulting coordination geometry can be described as a pseudo-trigonal bipyramid (Fig. 4(a)) or alternatively as a

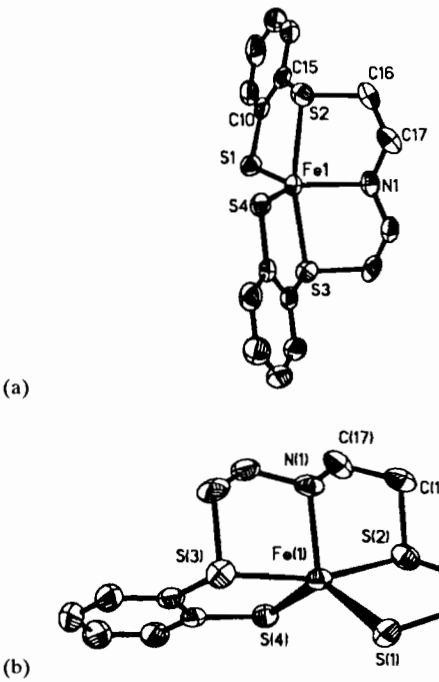

Fig. 4. Two views of the molecular structure of $[Fe('N_HS_4')]\cdot THF$ (**6**) (THF and H atoms omitted).

Table 6
Selected distances (pm) and angles (°) of $[Fe('N_HS_4')]\cdot THF$ (**6**)

Fe(1)–S(1)	230.4(2)	S(1)–Fe(1)–S(2)	86.1(1)
Fe(1)–S(2)	256.3(2)	S(1)–Fe(1)–S(3)	103.4(1)
Fe(1)–S(3)	251.8(2)	S(2)–Fe(1)–S(3)	165.4(1)
Fe(1)–S(4)	230.9(2)	S(1)–Fe(1)–S(4)	125.7(1)
Fe(1)–N(1)	214.3(5)	S(3)–Fe(1)–S(4)	86.6(1)
S(1)–C(10)	175.3(5)	S(1)–Fe(1)–N(1)	126.0(1)
S(2)–C(15)	178.2(7)	S(2)–Fe(1)–N(1)	81.9(1)
S(2)–C(16)	184.5(6)	S(3)–Fe(1)–N(1)	83.5(1)
N(1)–C(17)	147.9(7)	S(4)–Fe(1)–N(1)	108.0(1)

Table 7
Comparison of metal ligand distances (pm) in [Fe(CO)('N_HS_4')] [7], [Fe('N_HS_4')]·THF and [Fe(N_2H_4)('N_HS_4')] [4b]

	[Fe(CO)('N_HS_4')]	[Fe('N_HS_4')]·THF	[Fe(N_2H_4)('N_HS_4')]
d(Fe–thiolate-S)	229.8(3)	230.4(2)	238.1(3)
	230.5(3)	230.9(2)	240.2(3)
d(Fe–thioether-S)	222.5(3)	256.3(2)	260.2(3)
	225.1(3)	251.8(2)	260.2(3)
d(Fe–N)	207.2(8)	214.3(5)	225.5(6)

distorted square pyramid (Fig. 4(b)). Fig. 4(b) illustrates the close structural relationship of **6** to the chiral [Fe('N_HS_4')] core in low-spin [Fe(L)('N_HS_4')] complexes with L = CO, PR_3 or NO^+ where the thioether sulfur donors occupy *trans* positions.

With regard to the iron–donor distances, **6** takes an intermediate position between high-spin and low-spin [Fe(L)('N_HS_4')] complexes. As Table 7 shows, the Fe–S(thioether) and Fe–N(amine) distances are longer than in low-spin complexes but markedly shorter than in high-spin complexes, and the Fe–S(thiolate) distances are even as short as in low-spin [Fe(CO)('N_HS_4')].

The structure of **6** proves furthermore that coordinatively unsaturated 16 valence electron [Fe('N_HS_4')] fragments are stable in solution or solid state and do not dimerize via thiolate bridges.

In summary, **6** represents a kind of intermediate between high-spin and low-spin [Fe(L)('N_HS_4')] complexes. With regard to paramagnetism and high reactivity, it behaves like a high-spin complex, with regard to structure and bond lengths, it shows close resemblance to low-spin complexes.

4. Conclusions

The principal aim of this work was to find a method by which N_2 could be coordinated to the [Fe('N_HS_4')] fragment in order to obtain the N_2 complex which is the missing link in the series of N_2H_2, N_2H_4 and NH_3 complexes with the [Fe('N_HS_4')] core.

For this purpose, [Fe(L)('N_HS_4')] complexes with increasingly bulky phosphine ligands (L = PMe_3 (**1**), PMe_2Ph (**2**), PBu_3 (**3**) and $PMePh_2$ (**4**)) were synthesized and characterized. All phosphine complexes are chiral low-spin complexes. Corresponding to increasing cone angles and bulkiness of the phosphines, the Fe–P distances of the complexes elongate, the complexes become more labile, and particularly bulky phosphines like PPh_3 and PCy_3 did not coordinate to the [Fe('N_HS_4')] fragment. All phosphine ligands, including the small PMe_3, are labile and could easily be substituted by CO but not by the isoelectronic N_2.

The azido complex (NEt_4)[Fe(N_3)('N_HS_4')] (**5**), being another potential precursor for the N_2 complex, was synthesized and characterized by X-ray structure analysis. (NEt_4)[Fe(N_3)('N_HS_4')] (**5**) contains a high-spin Fe(II) center and an achiral [Fe('N_HS_4')] core. The azido ligand functions as a σ donor, is labile, and could not be converted into an N_2 ligand, neither by heating nor by oxidizing **5**. This is possibly due to the facile decoordination of the N_3^- ligand in solution, and furthermore to the achiral configuration and high-spin state of the [Fe('N_HS_4')] core both being unfavorable for the coordination of N_2.

If the azido ligand was transformed into an N_2 ligand, N_2 as σ–π ligand would require the chiral configuration and low-spin state of the [Fe('N_HS_4'] fragment in order to stay coordinated to the iron center. Thus isomerization of the [Fe('N_HS_4')] core would have to take place together with the $N_3^- \rightarrow N_2$ transformation, which, however, can presumably only be achieved via five-coordinate intermediates presupposing dissociation of at least one donor. The favorite candidate for dissociation, however, would be the N_2 ligand. Thus, configuration and the high-spin state of **5** may form a structural and electronic barrier to the $N_3^- \rightarrow N_2$ conversion.

Deprotonation of the amine donor in [Fe(CO)('N_HS_4')] did not labilize but strengthened the *trans* Fe–CO bond so that the CO ligand could not be cleaved off even photochemically. Formation of the [Fe(CO)('NS_4')]$^-$ anion was chemically confirmed by methylation yielding [Fe(CO)('$N_{Me}S_4$')] which contains an achiral *meso* [Fe('NS_4')] core.

[Fe('N_HS_4')]·THF (**6**) is a key complex concerning all reactions of the [Fe('N_HS_4')] system and formation of achiral high-spin complexes of type II with σ ligands or chiral low-spin [Fe(L)('N_HS_4')] complexes of type I with σ–π ligands. The starting compound for the syntheses of these complexes is usually [Fe(MeOH)('N_HS_4')] which has an achiral [Fe('N_HS_4')] core and a six-coordinate iron center. In order to explain the formation of either type I or type II complexes, decoordination of the MeOH ligand, and, in case of type I complexes, also isomerization of the [Fe('N_HS_4')] core, had to be postulated according to Scheme 1.

Isolation and full characterization of **6** have allowed Scheme 1 to be substantiated. [Fe('N_HS_4')]·THF (**6**) contains a five-coordinate iron center and can alter-

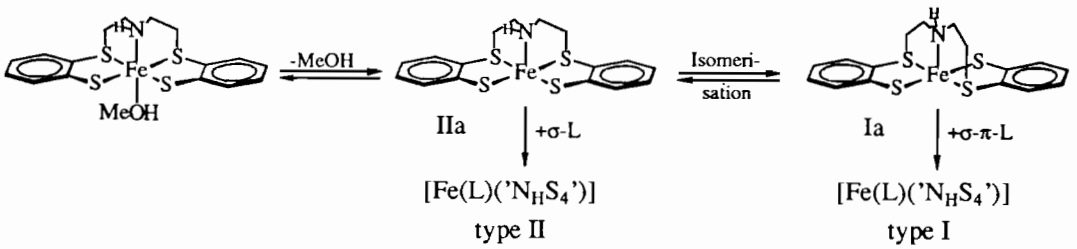

Scheme 1. Formation of achiral and chiral [Fe(L)('N_HS_4')] complexes.

natively be discussed as a distorted trigonal bipyramid or square pyramid. **6** represents a kind of intermediate between high-spin and low-spin [Fe('N_HS_4')] complexes. With regard to paramagnetism and reactivity **6** is a high-spin complex, with regard to structure and distances, it closely resembles low-spin complexes. Since trigonal bipyramidal or square pyramidal complexes with five-coordinate metal centers isomerize easily, **6** also corroborates the assumption that in solution an equilibrium between the two [Fe('N_HS_4')] fragments Ia and IIa exists which, upon reaction with the corresponding ligand L, gives either type I or type II [Fe(L)('N_HS_4')] complexes.

Finally, with respect to vacant sites of coordination, electronic versatility and structural flexibility, the [Fe('N_HS_4')] fragment exhibits properties which can also be expected from the iron centers in the active sites of nitrogenases.

Supplementary material

Further details of the X-ray structure analyses have been deposited and can be obtained from the Fachinformationszentrum Energie, Physik, Mathematik GmbH, D-76344 Eggenstein-Leopoldshafen, Germany, by citing the deposition No. CSD 400232 [Fe(PMe_2Ph)('N_HS_4')], CSD 400233 [Fe(PMe_3)('N_HS_4')], CSD 400234 [Fe(PBu_3)('N_HS_4')], CSD 400235 (NEt_4)[Fe(N_3)('N_HS_4')], CSD 400236 [Fe('N_HS_4')]·THF, the authors and reference.

Acknowledgements

We gratefully acknowledge support of these investigations by the Deutsche Forschungsgemeinschaft, the Bundesministerium für Forschung und Technologie, and the Fonds der Chemischen Industrie.

References

[1] D. Sellmann, Th. Hofmann and F. Knoch, *Z. Naturforsch., Teil B, 49* (1994) in press.
[2] (a) T.G. Spiro (ed.), *Metal Ions in Biology,* Vol. 4, *Iron Sulfur Proteins,* Wiley, New York, 1982; (b) T.G. Spiro (ed.), *Metal Ions in Biology,* Vol. 7, *Molybdenum Enzymes,* Wiley, New York, 1985; (c) T.R. Hawkes, P.A. McLean and B.E. Smith, *Biochem. J., 217* (1984) 217; (d) J.R. Lancaster (ed.), *The Bioinorganic Chemistry of Nickel,* Verlag Chemic, Weinheim, Germany, 1988.
[3] (a) M.M. Georgiadis, H. Komiya, P. Chakrabarti, D. Woo, J.J. Kornuc and D.C. Rees, *Science, 257* (1992) 1653; (b) J. Kim and D.C. Rees, *Science, 257* (1992) 1677.
[4] (a) D. Sellmann, W. Soglowek, F. Knoch and M. Moll, *Angew. Chem., 101* (1989) 1244; *Angew. Chem., Int. Ed. Engl., 28* (1989) 1271; (b) D. Sellmann, W. Soglowek, F. Knoch, G. Ritter and J. Dengler, *Inorg. Chem., 31* (1992) 3711.
[5] W. Wolfsberger and H. Schmidbaur, *Synth. React. Inorg. Met.-Org. Chem., 4* (1975) 149.
[6] W. Gee, R.A. Shaw and B.C. Smith, *Inorg. Synth., 9* (1967) 19.
[7] D. Sellmann, H. Kunstmann, F. Knoch and M. Moll, *Inorg. Chem., 27* (1988) 4183.
[8] C.A. Tolman, *Chem. Rev., 77* (1977) 313.
[9] (a) D. Sellmann, E. Licht, M. Moll and F. Knoch, *Z. Naturforsch., Teil B, 44* (1989) 429; (b) P.G. Douglas, R.D. Feltham and H.G. Metzger, *Chem. Commun.,* (1970) 889; (c) A.D. Allen, F. Bottomley, R.O. Harris, V.P. Reinsalu and C.V. Senoff, *J. Am. Chem. Soc., 89* (1967) 5595.
[10] (a) Z. Dori and R.F. Ziolo, *Chem. Rev., 73* (1973) 247; (b) U. Müller, *Struct. Bonding (Berlin), 14* (1973) 141.
[11] B.R. Cameron, D.A. House and A. McAuley, *J. Chem. Soc., Dalton Trans.,* (1993) 1019.
[12] M.L. Tobe, in A.G. Sykes (ed.), *Advances in Inorganic and Bioinorganic Mechanisms,* Academic Press, London, 1983, p. 1.
[13] D. Sellmann, Th. Becker, Th. Hofmann, F. Knoch and M. Moll, *Inorg. Chim. Acta, 219* (1994) 75.